encit 2020

ABCM Associação Brasileira de Engenharia e Ciências Mecânicas

18th Brazilian Congress of Thermal Sciences and Engineering
November 16–20, 2020 (Online)

# ENC-2020-0559
# HEAT TRANSFER INVESTIGATION FOR A MULTILAYER INSULATION SYSTEM VIA RADIATIVE-CONDUCTIVE APPROACH UNDER LOW TEMPERATURE CONDITIONS IN SPACE

**Guilherme Negreiros Lacerda**
**Marcos Filardy Curi**
Centro Federal de Educação Tecnológica Celso Suckow da Fonseca, Department of Mechanical Engineering, Rio de Janeiro, Rodovia Mário Covas, lote J2, quadra J, Rio de Janeiro, 23812-101,Brazil
gnegreiroslacerda@yahoo.com.br, marcos.curi@cefet-rj.br

***Abstract.*** *Thermal insulation is an important area, not restricted to mechanical engineering, but widely studied in environmental issues, such as global warming and, above all, energy-saving, since controlling the heat flux on microprocessors through temperature control on components in space applications. This work focuses on controlling the temperature in components that could not lose or gain so much heat in space, especially when the overall safety of sending satellites on specific missions is required. To ensure that, Multilayer Insulation (MLI) is used. With fluid mechanics and radiation-conduction heat transfer theory, it was possible to calculate the transient and stationary temperature field and heat flux in MLI. The boundary temperatures are specified at 300K and 4K. The results, from solving the resulting discretized ODE, simulated with fsolve and odeint Scipy subroutines in Python, able to solve the equations numerically, were shown. The data given by the simulation was able to indicate the impacts of varying the layer density, emissivity of screen, the distance between screens and the perforation coefficient in stationary and transient approaches. A way to simulate the performance of MLI numerically was presented. Modifying emissivity ($\varepsilon$) showed variations higher than in the perforation coefficient ($\xi$). Layer density controls the distance between layers ($\delta$), changing the conduction heat transfer. In the transient case simulation, it was possible to notice that varying parameters impact in time to reach steady-state and final temperature.*

***Keywords:*** *Heat Transfer, Numerical Analysis, Multilayer Insulation, Radiative-conductive approach*

## 1. INTRODUCTION

In 1900 the first experiment involving Multilayer Insulation was made by Sir James Dewar using three layers of alumminum foil. On the other hand, only in 1947 (Cornell, 1947) made a detailed discrimination of a radiation shield system. (Black *et al.*, 1959) have done an important study in the area, considering radiation, solid and gas conduction, and proposed formulation for each heat transfer. The work of (MacGregor *et al.*, 1970) takes into consideration the specular diffuse reflection. The first work that investigate perforated MLI was (Tien and Cunnington, 1973), where a different formulation was given due to perforation's coefficient. (Keller *et al.*, 1974) made an important report requested from NASA studying the heat transfer in MLI with several experiments and variations in design.

Nowadays, in areas where the thermal insulation is essential, it is possible to see many spacecrafts coated with MLI blankets due to your great capacity for insulation - composed of several layers of low-emittance films and lightweight. In that sense, becoming an essential passive thermal control in spacial applications. In the beginning, the blankets were thought and produced only to avoid heat flux going in and out of the spacecraft. Today, they can guarantee protection for micrometeoroids, atomic oxygen, electron charge accumulation and rocket-engine plume impingement. Also, they require durability, flammability, contamination control, launch loads, pressure decay, spacecraft venting, glint minimization, and restrictions on magnetic materials (Gilmore, 2001).

According to (Meseguer *et al.*, 2012), to calculating the heat transfer through MLI is necessary a combination of radiation, solid conduction, and, under atmospheric conditions, gaseous conduction. Each form of heat transfer is reduced differently. To minimize radiation heat transfer, a large number of reflective surfaces are confined to isolate the object. Solid-conduction heat transfer could be decreased by making the low-conductance spacer's density between the reflective surfaces as low as possible and avoiding contact between layers. Gaseous-conduction heat transfer is reduced by doing the insulation to vent to space after the vehicle is launched.

Several parameters should be known to calculate MLI's effective thermal conductivity, like the shield and spacer material's properties, the number of layers and layer density, contact pressure, vacuum maintained and interstitial pressure. (Bapat *et al.*, 1990) shows several analytical and empirical equations developed by various investigators. Taken the methods used by (Zhitomirskij *et al.*, 1979), (Bapat *et al.*, 1990) and (Li and Cheng, 2006b) for the densities of the

incident radiant flows. To calculate the heat transfer problem, using the energy balance for each node, Fourier's Law and Stefan-Boltzmann's Law can reach the temperature profile equation.

Studies in the 2010's are more focused on variations on the design. (Dye *et al.*, 2010) designed two new spacers made of polymer for MLI, one that makes possible control the layer spacing and the other where the spacer would support the load. (Johnson, 2010) made his master thesis concerning on various layer spacings and its impacts on the thermal behaviour of MLI. In their method, (Johnson *et al.*, 2017) have considered the material's transmissivity and made several tests, (Mazzinghi *et al.*, 2018) designed a special MLI with RF behavior maximized. (Miyakita *et al.*, 2019) developed a new MLI using a non-interlayer-contact spacer and performed experiments to ensure their new MLI's performance still under atmosphere going to a vacuum. (Wang *et al.*, 2019) studied how to optimize MLI production, reducing the differences between the designs, increasing MLI fabrication efficiency.

This research aims to analyse the influence of some parameters in the performance of MLI thermal insulation. Testing modifications in different materials and aspects of construction, such as emissivity, the material reflective perforated and the distance between the materials. Governing equations from radiation-conduction heat transfer problems were used in modelling the mathematical formulation. Nevertheless, it is worth to mention that numerical data, by the approach proposed here, is not simple to find either. However, the experimental procedure for this subject has an extensive literature.

An algorithm in Python solved the equations of the problem in each case. Most research in literature has simplified the conduction-radiation equations due to all the equation's complexity (several coupled non-linear differential equations) In this paper, this type of simplifications was minimized. Moreover, clearly given a form to predict the behavior of MLI numerically with accuracy is extremely important.

## 2. PROBLEM FORMULATION AND SOLUTION METHODOLOGY

The MLI consists of perforated isothermal reflective screens and spacer with low conductance fixed between them, Figure 1. The "cold" and "warm" boundary temperature are Tc and Th, respectively. The warm boundary is the spacecraft, maintaining any electronic component's operational temperature, or for the crew into the spacecraft. The cold boundary is the space itself. There are N layers in the system.

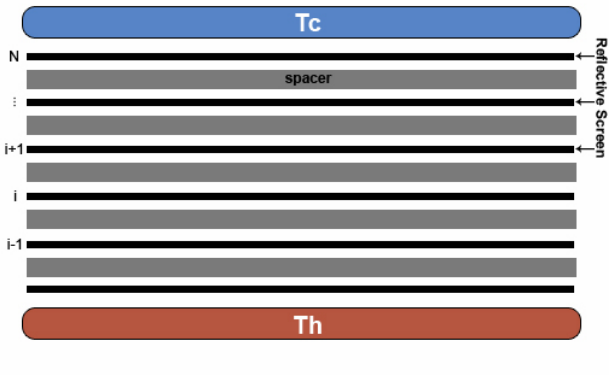


Figure 1. A model of the MLI.

### 2.1 General Formulation

The problem is governed by a discretized transient one-dimensional ODE for each node, Figure 2, expressed by:

$$\mathbf{c_i}\rho_i\frac{\mathbf{dT_i}}{\mathbf{dt}} = \xi_i'\varepsilon_i(\mathbf{F_{1,i}} + \mathbf{F_{2,i}} - \mathbf{2}\sigma\mathbf{T_i^4}) + \mathbf{k_{eq,i}}\frac{\mathbf{T_{i-1}} - \mathbf{T_i}}{\delta_i} + \mathbf{k_{eq,i+1}}\frac{\mathbf{T_{i+1}} - \mathbf{T_i}}{\delta_{i+1}} \tag{1}$$

Where $c$ is heat capacity, $\rho$ is density of reflective screen and $\delta$ is the distance between the screens, $\xi$ is the perforation coefficient, $\xi'$ is $(1-\xi)$, $F_1$ e $F_2$ the radiation flux in a node. Figure 2 show the flux of the heat, where $F_1$ and $F_2$ are the flux of radiation in the screen, and $q_c$ is the heat flux by solid and gas conduction.

This work also studied the steady-state of the problem. Besides the simplicity of the formulation, it shows the temperature field's final values and would be useful to compare with the expected transient behavior. The equation in each node is given by:

$$\xi_i'\varepsilon_i(\mathbf{F_{1,i}} + \mathbf{F_{2,i}} - \mathbf{2}\sigma\mathbf{T_i^4}) + \mathbf{k_{eq,i}}\frac{\mathbf{T_{i-1}} - \mathbf{T_i}}{\delta_i} + \mathbf{k_{eq,i+1}}\frac{\mathbf{T_{i+1}} - \mathbf{T_i}}{\delta_{i+1}} = 0 \tag{2}$$

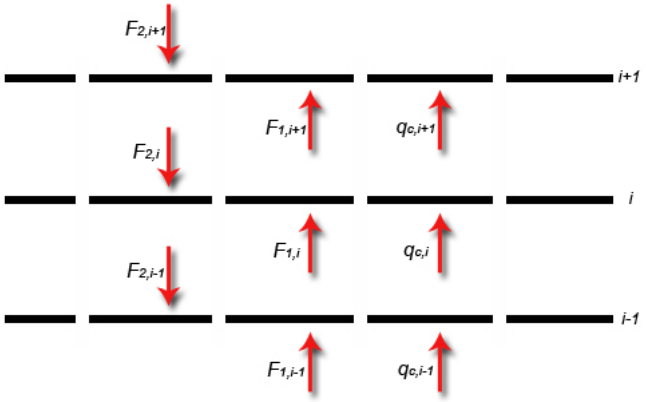


Figure 2. The radiation heat flux.

### 2.2 Incident Radiation Flux

Taking the flow coming in the each layer from both sides Figure 2, the equations are:

$$\mathbf{F_{2,i-1}} = \xi_\mathbf{i}\mathbf{F_{2,i}} + \xi'_\mathbf{i}\varepsilon_\mathbf{i}\sigma\mathbf{T_i^4} + \xi'_\mathbf{i}\varepsilon'_\mathbf{i}\mathbf{F_{1,i}} \tag{3}$$

$$\mathbf{F_{1,i}} = \xi_\mathbf{i-1}\mathbf{F_{1,i-1}} + \xi'_\mathbf{i-1}\varepsilon_\mathbf{i-1}\sigma\mathbf{T_{i-1}^4} + \xi'_\mathbf{i-1}\varepsilon'_\mathbf{i-1}\mathbf{F_{2,i-1}} \tag{4}$$

Where $\varepsilon$ is the emissivity of the material and $\varepsilon'$ is $(1-\varepsilon)$.

### 2.3 Thermal Conductivity

The thermal conductivity is important in the process, adding the radiation flux for the heat transfer. In perforated MLI, the gas thermal conductivity makes a difference, becoming the sum of the solid and gas thermal conductivity. In the simplest case, whith no perforation, only the solid thermal conductivity matters.

#### 2.3.1 Solid Thermal Conductivity

The most common spacer used is the glass fibres and its thermal conductivity $k_{sp}$ was obtained by a semi-empirical method in (Zhitomirskij *et al.*, 1979):

$$\mathbf{k_{sp}} = \mathbf{An^K k_g(T)} \tag{5}$$

Where *A* and *K* are empirical coefficients, *A* depends on *n*, and *n* is the layer density.

$$\mathbf{k_g(T)} = \mathbf{0.22 + 0.26 * T * 10^{-2}} \tag{6}$$

The temperature in (5) is the arithmetic average between the temperatures of the screens around the spacer. This formula is given by (Mazurin *et al.*, 1983).

The contact thermal conductivity between the spacer and the screen is:

$$\mathbf{H} = \mathbf{2}\xi'\mathbf{r k_m} \tag{7}$$

Where r is the contact radius between spacer and screen, $k_m$ is the thermal conductivity equivalent of the screen and the spacer, both given by:

$$\mathbf{r} = (\mathbf{0.75}\pi(\mathbf{K_{sc}} + \mathbf{K_{sp}})\mathbf{P t_p}/\mathbf{N_T^2})^{\mathbf{1/3}} \tag{8}$$

$$\mathbf{k_m} = \mathbf{2k_{sc}k_{sp}}/(\mathbf{k_{sc}} + \mathbf{k_{sp}}) \tag{9}$$

where $k_{sp}$ and $k_{sc}$ are the thermal conductivity of the spacer and the screen, respectively.

The solid equivalent thermal conductivity between the screens is:

$$\mathbf{k_{eq,s}} = \frac{\delta}{\mathbf{1/H} + \delta/\mathbf{k_{sp}}} \tag{10}$$

### 2.3.2 Gas Thermal Conductivity

In the case of the perforated screen, the gas thermal conductivity is used and given by: (Chen *et al.*, 1994):

$$\mathbf{k_{eq,g}} = \mathbf{a}\nu\mathbf{R}\mathbf{N}^{\mathbf{2}}\frac{\xi'}{\xi}\delta_{\mathbf{t}} \tag{11}$$

where $a$ is accommodation coefficient, $\nu$ is the outgassing rate in one side of the screen, $R$ is the gas constant, $\delta_t$ is total thickness of the MLI and $N$ is the number of layers.

The outgassing rate of the material, defined as the mass of gas per area going out in time, is given by:

$$\nu = \nu_{\mathbf{0}}\frac{\mathbf{T_0}}{\mathbf{T}}\mathbf{e}^{-(\mathbf{E_d}/\mathbf{2R})(\mathbf{1}/\mathbf{T}-\mathbf{1}/\mathbf{T_0})} \tag{12}$$

where $\nu_0$ is the outgassing rate at the temperature $T_0$, $E_d$ is the activation energy for diffusion.

### 2.3.3 Effective Thermal Conductivity

Been effective thermal conductivity the sum of the solid and gas conductivity:

$$\mathbf{k_{final}} = \mathbf{k_{eq,s}} + \mathbf{k_{eq,g}} \tag{13}$$

## 2.4 Solution Methodology

Figure 3 is a diagram that shows the process of the programs. The initial conditions are the proprieties of materials, physical constants and other MLI parameters. The initial temperatures of layers were set as 300K. As the first stage of the simulation in the stationary case, with the input set's values, the initial thermal conductivity is calculated, then the radiation flux can be calculated using Eq. (3) and Eq. (4).

After that, the temperatures are recalculated by Eq. (2), and then new thermal conductivity and radiation heat flux are obtained again. This process was repeated several times until the difference of the new temperature and the temperature of the previous step became less then $0.001$.

It was necessary to use a solver in Python to optimize this process called *fsolve* from a free library Scipy. As mentioned above, the boundaries temperatures were set, where the surface of the spacecraft was 300K, and the space temperature was 4k.

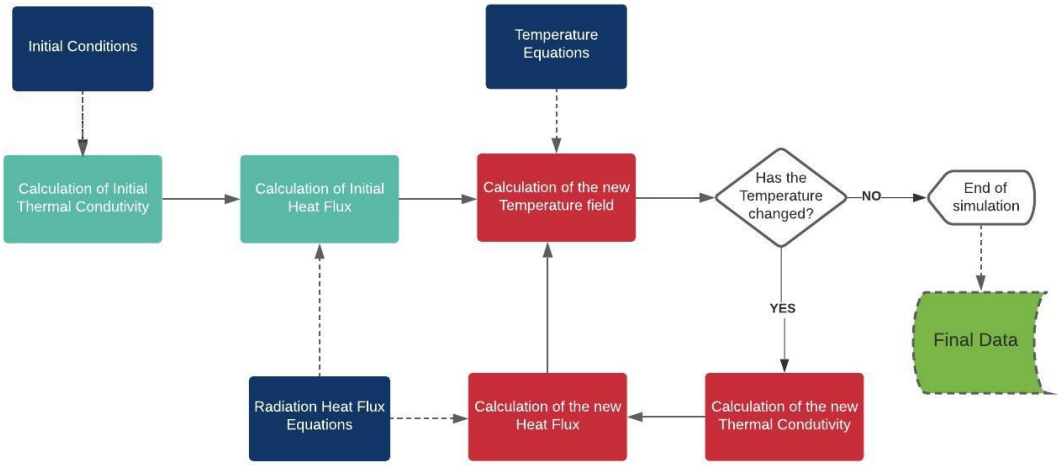


Figure 3. The entire process of Stationary problem.

In transient cases, the process is similar, Eq. (1) is used instead of Eq. (2) for the temperature field, for each layer was used a solver for ODE in python named *odeint* from Scipy either. Every step in the solution that radiation heat flux was updating the ODE's referent, the temperatures were solved in 4000 points with the time step approximately 0.045s. Although the time considered not progress only summing the time step, in each solution of ODE is taken the temperature in the next point, the next time is the sum of time already been simulated and the time of temperature taken.

## 3. RESULTS AND DISCUSSIONS

Fig. 4 shows the comparison between the heat flux through the MLI calculated, and with data from (Krishnaprakas *et al.*, 2000), their work showed an experimental correlation and then compared with methods to calculate the heat flux

analytically. The line from this research is very similar to the experimental data. All parameters used in their experiment is not completely described. Using the criterion specified was possible to show the convergence of heat flux behaviour, varying the hot temperature. The cold temperature was 173K. It is possible to note a similar behavior from this work and with those presented by (Krishnaprakas *et al.*, 2000). The graphical displacement is due exactly to the mentioned parameters that were not fully informed. However, given the high complexity of the theoretical formulation, a good agreement of the results for the heat flux could be noted.

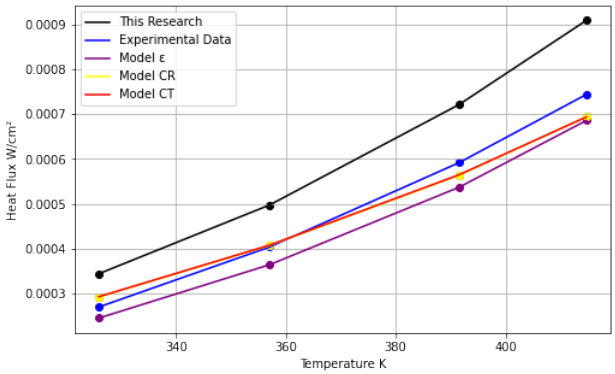


Figure 4. Comparison between the data of heat flux.

### 3.1 Stationary

Layer density variation results in different effective thermal conductivities, $k_{final}$, and heat loss flux. (Li and Cheng, 2006b) showed that in around 18 to 24 layer density is found the minimum of $k_{final}$. (Jacob *et al.*, 1992) have done several experiments on the effective thermal conductivity according to layer density. Figure 5 shows the number of layers and the temperature in each layer. From Fig. 5, every black dot for a specific layer density is equivalent to a node, i.e., the respective reflective screen between Tc and Th. Note that when increasing the layers, the final temperature in the last layer decreases until around a minimum for $k_{final}$, then when the number of layer keep increasing, the temperature of the last layer also start to increases. The perforation coefficient was set as $\xi = 1.4\%$, the emissivity of the screen and surface of satellite respectively $\varepsilon_{sc} = 0.2$, $\varepsilon_{su} = 0.05$. Vary layer density impact in changing the $\delta$. As increasing layer density, the heat conduction becomes higher and heat radioactive smaller.

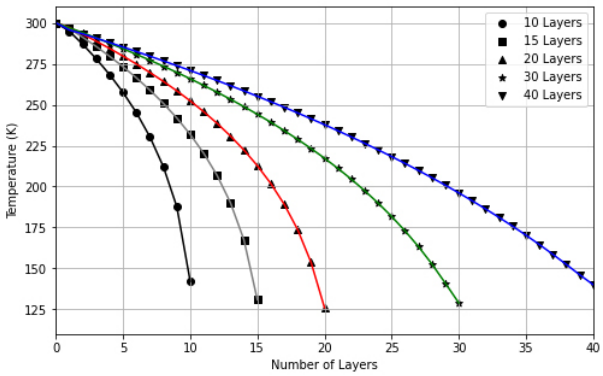


Figure 5. Variation in number of layers and its impact in final temperatures.

The results in Tab. 1 shows the temperature of the last layer for each layer density. It can be noticed that the optimum layer density, where optimize the heat loss, around $n$ = 20, with the lowest temperature.

The modification in $\delta$, the distance between the screens, impacts Eq. (1) and Eq. (2), influencing the heat conduction as shown in the equations. Figure 6 and Tab. 2 is the result of a variation in $\delta$ for 20 layers case. Tab. 1, compares the results of $\delta$ fixed and variable, the first variation is making the first $\delta$ the same as the fixed, and the second adding 30% of the first $\delta$, and the third adding 30% of the second, and this continues until the last $\delta$. The second variation is the same, but adding 50% in each step. The third is equal the last two, but now decreasing 5%. Those data shows the importance of the $\delta$ in the process, making the temperature higher in 7.32%. When the distance is decreasing by 5%, consequently, the heat loss is higher.

Figure 7 depicts the temperature distribution for $n$=20, zoomed in for capture its sensitive variation. The graph on the left shows the impact in the temperature field due to the $\xi$ variation. The right one shows the variation in $\varepsilon$. It is possible

Table 1. Final temperature of the last Layer

| Number of Layers | Temperature of the last layer (K) |
|---|---|
| 10 | 142.166 |
| 15 | 130.926 |
| 20 | 126.097 |
| 30 | 129.002 |
| 40 | 140.171 |

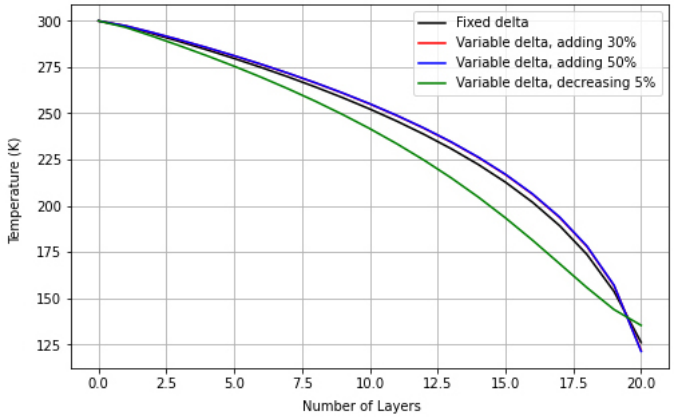


Figure 6. Variation in $\delta$ and its impact in final temperatures.

Table 2. Variable $\delta$ and the temperatures.

| Distance (m) | Temperature of the last layer (K) |
|---|---|
| 5.2x10$^{-4}$ | 126.097 |
| Adding 30% | 121.744 |
| Adding 50% | 121.285 |
| Decreasing 5% | 135.335 |

to note when increasing the $\xi$ the temperature is higher. And increasing $\varepsilon$ occurs a inversion of the temperature in the last 2 layers. It is possible to note that, increasing $\varepsilon$ the material reflect less heat, this explain the behavior of Fig.7(right). Varying $\xi$ impacts directly on the thermal conductivity, Eq. (11). The contribution of Eq. (11) in $k_{final}$ is little, showing the poor impact in Fig.7(left) of temperature field.

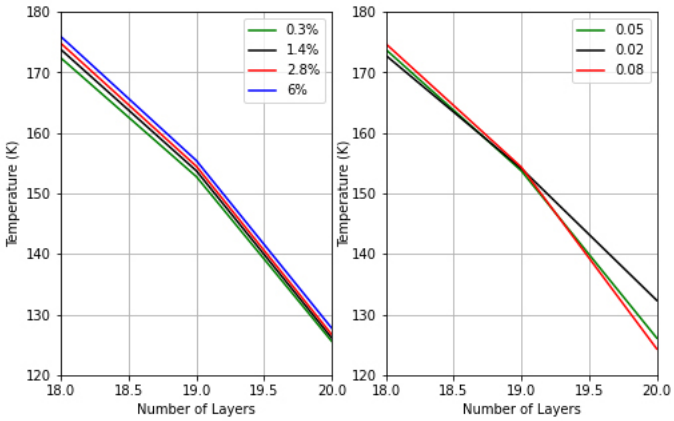


Figure 7. Variation in $\xi$ (left) and $\varepsilon$ (right).

### 3.2 Transient

In Figure 8 the perforation coefficient was set as $\xi = 3\%$, the emissivity of the screen and the surface of the satellite respectively $\varepsilon_{sc} = 0.2$, $\varepsilon_{su} = 0.05$. Figure 8 shows a comparison of data given by the simulation and from (Li and Cheng, 2006a). It could be noted that the data are homogeneous. Due the omitted parameters by (Li and Cheng, 2006a), the graphs are close enough to ensure that the lines have the same pattern.

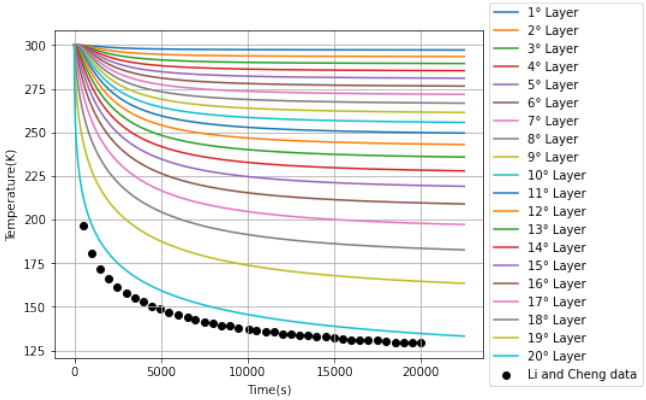


Figure 8. Comparison between the data of transient heat transfer.

Figure 9 exhibit the behavior of variation in $\varepsilon$, the impact in transient heat transfer is notorious. As $\varepsilon$ increases the last layer final temperature is lower, and also reach the steady-state faster. In the first layer temperature has no change considerable.

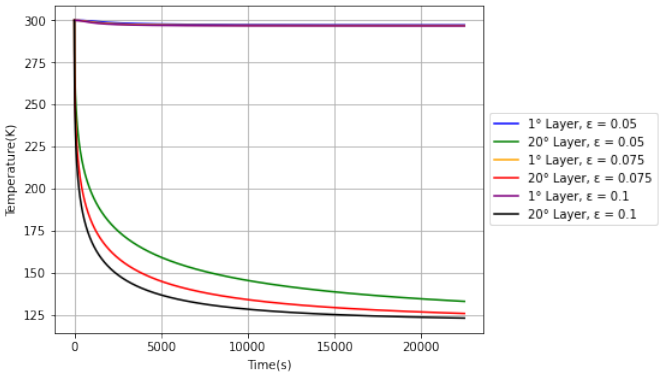


Figure 9. Results of variation in $\varepsilon$.

Figure 10 exhibit the behavior of variation in $\xi$. It is possible to notice that varying $\varepsilon$ has more results then in $\xi$, also shown in Figure 7.

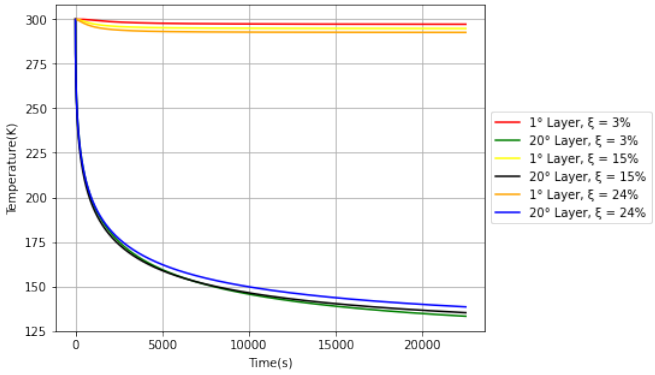


Figure 10. Results of variation in $\xi$.

## 4. CONCLUSIONS

A one-dimensional formulation for transient and stationary heat transfer problems for perforated MLI with set boundary conditions is presented. The formulation includes a non-linear ODE for radiative-conductive problem. The methodology employed presented good results compared with the actual literature, guaranteeing the developed code validation. Some parameters of the MLI have great importance to control in each case. Results for the transient and steady-state temperature profile for each variation of the following parameters, $\varepsilon$, $\xi$, and $\delta$, were presented. It is verify that:

- It is possible to make a good numerically prediction of temperature field and heat flux.
- In transient or stationary case is possible notice that the impact of varying $\varepsilon$ is bigger than $\xi$.
- Layer density is a crucial variable, it controls the distance between the reflective materials and also make changes in thermal conductivity.
- Variations in transient case show that is possible reach the steady-state faster and also a lower final temperature.

## 5. REFERENCES

Bapat, S.L., Narayankhedkar, K.G. and Lukose, T.P., 1990. "Performance prediction of multilayer insulation". *Cryogenics*, Vol. 30, pp. 700–710.

Black, J.A., Fowle, A.A. and Glasser, P.E., 1959. "Development of high efficiency insulation". *Advances in Cryogenic Engineering*, Vol. 5, pp. 181–188.

Chen, G., Sun, T., Zheng, J., Huang, Z. and YU, J., 1994. "Performance of multilayer insulation with slotted shield". *Cryogenics*, Vol. 34, pp. 381–384.

Cornell, W.D., 1947. "Radiation shield supports in vacuum insulated containers". *US Patent*, Vol. 2.643.022.

Dye, S., Kopelove, A. and Mills, G.L., 2010. "Integrated and load responsive multilayer insulation". *Advances in Cryogenic Engineering*, Vol. 55, pp. 946–953.

Gilmore, D.G., 2001. *Spacecraft Thermal Control Handbook*. The Aerospace Corporation, California, 2nd edition.

Jacob, S., Kasthurirengan, S. and Karunanithi, R., 1992. "Investigations into the thermal performance of multilayer insulation (300- 77 k) part 2: Thermal analysis". *Cryogenics*, Vol. 32, pp. 1147–1153.

Johnson, W.L., 2010. *Thermal Performance of Cryogenic Multilayer Insulation at various Layer Spacings*. Master's thesis, University of Central Florida, Florida, USA.

Johnson, W.L., Dresar, N.T.V., Chato, D.J. and Demers, J.R., 2017. "Transmissivity testing of multilayer insulation at cryogenic temperatures". *Cryogenics*, Vol. 86, pp. 70–79.

Keller, C.W., Cunnington, G.R. and Glassford, A.P., 1974. "Thermal performance of multilayer insulations". *NASA CR-134477*.

Krishnaprakas, C.K., Narayana, K.B. and Dutta, P., 2000. "Heat transfer correlations for multilayer insulation systems". *Cryogenics*, Vol. 40, pp. 431–435.

Li, P. and Cheng, H., 2006a. "Numerical simulation of multilayer perforated insulation material using in space". *AIAA/ASME Joint Thermophysics and Heat Transfer Conference*, Vol. 9.

Li, P. and Cheng, H., 2006b. "Thermal analysis and performance study for multilayer perforated insulation material used in space". *Applied Thermal Engineering*, Vol. 26, pp. 2020–2026.

MacGregor, R.K., Pogson, J.T. and Russell, D.J., 1970. "Radiation interchange interior to multilayer insulation blankets". *Journal of Spacecraft and Rockets*, Vol. 7:2, pp. 221–223.

Mazurin, O.V., Streltsina, M.V. and Shvaiko, T.P., 1983. *Handbook of Glass Data*. Elsevier Science Publishing Company, New York, volume 15, part a edition.

Mazzinghi, A., Sabbadini, M. and Freni, A., 2018. "Enhanced rf behavior multi-layer thermal insulation". *Scientific Reports*, Vol. 8.

Meseguer, J., Pérez-Grande, I. and Sanz-Andrés, A., 2012. *Spacecraft thermal control*. Woodhead publishing, Cambridge, first edition edition.

Miyakita, T., Kitamoto, K., Kinefuchi, K., Sugita, H., Saitoh, M. and Hirai, T., 2019. "Development of a new mli for orbital cryogenic propulsion systems -thermal performance under one atmosphere to a vacuum". *IOP Conf. Series: Materials Science and Engineering*, Vol. 502, pp. 1–5.

Tien, C.L. and Cunnington, G.R., 1973. "Radiation heat transfer in multilayer insulation having perforated shields". *AIAA Thermophysics Conference*, Vol. 8, pp. 1–5.

Wang, Z., Fu, H. and Fan, Z., 2019. "Research on the production mode of improving production efficiency of spacecraft multi-layer insulation". *Advances in Engineering Research*, Vol. 184, pp. 45–49.

Zhitomirskij, I.S., Kislov, A.M. and Romanenko, V.G., 1979. "A theoretical model of the heat transfer processes in multilayer insulation". *Cryogenics*, Vol. 19, pp. 265–268.

## 6. RESPONSIBILITY NOTICE

The authors are solely responsible for the printed material included in this paper.